



Published in final edited form as:

Nat Microbiol. 2020 February ; 5(2): 368–378. doi:10.1038/s41564-019-0641-0.

Diet-derived galacturonic-acid regulates virulence and intestinal colonization in enterohemorrhagic *E. coli* and *Citrobacter rodentium*.

Angel G. Jimenez^{1,2}, Melissa Ellermann^{1,2}, Wade Abbott^{3,4}, Vanessa Sperandio^{1,2,*}

¹Department of Microbiology, University of Texas Southwestern Medical Center, Dallas, TX 75390-9048, USA

²Department of Biochemistry, University of Texas Southwestern Medical Center, Dallas, TX 75390-9048, USA

³Lethbridge Research and Development Centre, Agriculture and Agri-Food Canada, Lethbridge, Alberta, Canada

⁴Department of Chemistry and Biochemistry, University of Lethbridge, Lethbridge, Alberta, Canada

Abstract

Enteric pathogens sense the complex chemistry within the gastrointestinal (GI) tract to efficiently compete with the resident microbiota and establish a colonization niche. Here we show that enterohemorrhagic *E. coli* (EHEC), and its surrogate murine infection model *Citrobacter rodentium*, sense galacturonic-acid to initiate a multi-layered program towards successful mammalian infection. Galacturonic-acid utilization as a carbon source aids the initial pathogen expansion. The main source of galacturonic-acid is dietary pectin, which is broken into galacturonic-acid by the prominent member of the microbiota, *Bacteroides thetaiotaomicron* (*Bt*). This regulation occurs through the ExuR transcription factor. However, galacturonic-acid is also sensed as a signal through ExuR to modulate the expression of the genes encoding a molecular syringe known as a type three secretion system (T3SS) leading to infectious colitis and inflammation. Galacturonic-acid moonlights as a nutrient and a signal directing the exquisite microbiota-pathogen relationships within the GI tract. Importantly, this work highlights that differential dietary sugar availability impacts the relationship between the microbiota and enteric pathogens, as well as disease outcomes.

Users may view, print, copy, and download text and data-mine the content in such documents, for the purposes of academic research, subject always to the full Conditions of use:http://www.nature.com/authors/editorial_policies/license.html#terms

*Correspondence should be sent to: Vanessa Sperandio, Ph.D., University of Texas Southwestern Medical Center, Dept. of Microbiology, 5323 Harry Hines Blvd. Dallas, TX 75390-9048, USA, Telephone: 214 648 5619, Fax: 214 648 5905, vanessa.sperandio@utsouthwestern.edu.

Author contributions

AGJ conceived the studies, performed experiments and data analysis and wrote the paper. ME performed histological analysis, performed some mouse experiments. WA advised on experiments with *Bacteroides thetaiotaomicron* and pectin degradation. VS supervised all experiments, analyzed data, and wrote the paper.

Competing interests

The authors have no competing interest.

Keywords

enterohemorrhagic *E. coli* (EHEC); ExuR; glucuronate; galacturonate

The mammalian GI tract is populated by a dense and highly adapted microbiota. Glycan foraging plays a key role in the establishment and maintenance of these microbial communities¹. Bacterial pathogens have evolved metabolic adaptations and elaborate virulence mechanisms to effectively compete with commensal microbes². EHEC has a very low infectious dose, estimated to be 50 colony forming units (CFU)³. Inasmuch as EHEC's colonization site within the GI tract is the colon, which is one of the most heavily colonized regions by the microbiota³, EHEC has to be an extremely efficient pathogen to gain a foothold within the gut.

The microbiota poses a significant barrier to enteric pathogens. EHEC and *C. rodentium* (a murine pathogen extensively used as a surrogate model for EHEC infection⁴) can overcome this barrier by deploying their T3SSs⁵. T3SSs are molecular syringes employed by many Gram-negative pathogens to translocate their repertoire of effector proteins into the host cell. These effectors either hijack or mimic eukaryotic cell function benefiting the pathogen⁶. The genes encoding EHEC's and *C. rodentium*'s T3SSs are contained within a pathogenicity island named the locus of enterocyte effacement (LEE)^{7,8}. Expression of the LEE in *C. rodentium* is downregulated by 21 days post-infection, and the pathogen is quickly outcompeted by the microbiota and cleared from the intestine⁵. The ability of the microbiota to outcompete *C. rodentium* is dependent on nutrient availability. Saccharolytic members of the microbiota, such as *Bt*, which can break down and utilize complex carbohydrates, do not compete with *C. rodentium* for nutrients⁵. However, commensal *E. coli*, which can only utilize mono and di-saccharides, are direct competitors, resulting in the ultimate clearance of the pathogen⁵.

EHEC and commensal *E. coli* strains utilize overlapping and distinct sugars to establish and maintain host colonization⁹⁻¹². Notably, catabolism of sucrose and galacturonic and glucuronic-acids, but not gluconate is important for colonization by EHEC, while commensal *E. coli* strains use gluconate but not galacturonic and glucuronic-acids, suggesting that EHEC has evolved different nutritional requirements from its closely related commensal *E. coli*¹¹. Galacturonic-acid is a dietary-derived metabolite that is necessary for the establishment of pathogenic strains of *E. coli* in the gut^{9,10}. EHEC metabolizes this sugar using the Ashwell pathway, which is under the control of the ExuR transcriptional regulator^{9,10}. A high throughput screen for metabolic pathways and transcriptional factors that regulate LEE gene expression identified ExuR as a LEE regulator¹³. ExuR is a member of the GntR family of transcriptional regulators¹⁴, has been previously characterized as a regulator of sugar acid catabolism in *E. coli*^{15,16}, and is responsive to galacturonic-acid¹⁷⁻¹⁹.

Here we show that the ExuR regulon comprises the galacturonic-acid utilization genes and the LEE. We show that galacturonic-acid utilization as a carbon source aids pathogen expansion only in the beginning of infection. Moreover, ExuR, in the absence of galacturonic-acid, as infection proceeds, acts as an activator of the LEE genes leading to

colitis and inflammation. Altogether, ExuR orchestrates enteric pathogenesis by shifting its role as a regulator of metabolism and virulence in the context of microbiota and diet.

Results

ExuR directly regulates LEE gene.

A screen to identify genes that impact LEE gene expression identified ExuR as a LEE regulator¹³. ExuR is a transcription factor that regulates sugar acid metabolism in *E. coli* K12^{9,10}. To assess if the Ashwell pathway is regulated by ExuR in EHEC and to corroborate the findings of our screen, we generated an isogenic *exuR* EHEC mutant. Transcriptomic (European Nucleotide Archive accession number: PRJEB30676) and targeted qRT-PCR analysis confirmed that ExuR regulates the Ashwell pathway and the LEE in EHEC (Fig. 1a and Extended Fig.1). Deletion of *exuR* led to a significant decrease in transcript levels of LEE-encoded genes (*ler*, *espA*, and *tir*) (Fig. 1c–e), and proteins grown in DMEM in the absence of galacturonic-acid (Fig. 1f). An *in silico* search for the ExuR DNA binding consensus sequence (Fig. 1g)¹⁴; found a potential binding site within the regulatory region of the *ler* gene. The LEE harbors 41 genes, the majority of which are organized in five operons named *LEE1–5*³. *Ler* is encoded by the first gene within the *LEE1* operon, and is the activator of all of the LEE genes²⁰ (Fig. 1b). *LEE1* in EHEC has two promoters, P1 and P2²¹, and the ExuR DNA binding consensus sequence is upstream of P1 (Fig. 1h). ExuR directly binds to the *ler* regulatory region (Fig. 1i and Extended Data Fig. 1c) to activate *ler* transcription, and consequently LEE gene expression (Fig. 1c–e). The LEE-encoded T3SS promotes the formation of attaching and effacing (AE) lesions on epithelial cells. These lesions lead to effacement of the microvilli, and rearrangement of the host cell actin, forming pedestal-like structures underneath the attached bacteria³. Congruent with the decreased expression of the LEE genes, *exuR* forms fewer AE lesions than the wild-type (WT) and complemented strains (Fig. 1j,k).

Sensing of galacturonic-acid decreases expression of the T3SS and is dependent on ExuR.

E. coli can transport and utilize galacturonic and glucuronic-acids as carbon sources¹⁰. ExuR controls the transport and catabolism of sugar acids (*uxaABC*, *uxuAB*, *uxuR* and *exuT* genes). In the absence of galacturonic-acid, ExuR represses transcription of the *uxaAC*, *uxuAB*, *uxuR* and *exuT* genes, and activates LEE expression (Fig. 1a and Extended Data Fig.1a)^{9,10}. Galacturonic-acid binds to ExuR and hinders its ability to interact with DNA^{9,10}. Consequently, in the presence of galacturonic-acid the genes necessary for its utilization are expressed^{9,10}, and the LEE genes are repressed (Fig. 2a–c). Importantly, galacturonic-acid repression of the LEE is ExuR-dependent (Fig. 2d,e). Of note, the LEE is also present in enteropathogenic *E. coli* (EPEC), and its regulation is similar to EHEC³, consequently, galacturonic-acid also represses LEE gene expression in EPEC (Extended Data Fig. 3d). An EHEC *uxaC* (*UxaC* encodes the first enzyme in galacturonic-acid utilization (Fig. 5a)) can't grow in minimal media when glucuronic or galacturonic-acid is a sole carbon source (Extended Data Fig. 2a). However, it can grow in low glucose DMEM in the absence or presence of galacturonic-acid (Extended Data Fig. 2a,c). Growth of EHEC in low glucose DMEM is conducive to LEE gene expression *in vitro*^{7,22}. To probe whether galacturonic-

acid LEE gene regulation was dependent on it being utilized as a carbon source or as a signal, we titrated the concentration of this sugar to levels in which it no longer was used for growth (Extended Data Fig. 2c). At a concentration of 100 μ M, galacturonic-acid does not contribute to EHEC's growth (Extended Data Fig. 2c), but still serves as a signal to decreased LEE-gene expression (Fig. 2e). These data suggest that galacturonic-acid serves as both a nutrient and a signal to modulate gene expression.

ExuR is important for *C. rodentium* murine pathogenesis.

EHEC is a human pathogen and therefore EHEC murine models of infection fail to recapitulate several of the key features of EHEC pathogenesis. These include AE lesion formation, induction of inflammation and mucosal colonization. *C. rodentium* has been used extensively as a model of EHEC infection²³. *C. rodentium* harbors the LEE and forms AE lesions in the colon of mice²³. Importantly, LEE regulation by ExuR is conserved between EHEC and *C. rodentium* (Extended Data Fig. 3a,b). To investigate the role of ExuR during murine infection, C3H/HeJ mice (this strain of mice is more susceptible to *C. rodentium* infection and succumb to death⁴) were orally inoculated with wild-type (WT) *C. rodentium* DBS100 or with an *exuR* isogenic mutant. Mice that were infected with WT *C. rodentium* completely succumbed to the infection by day 11. However, mice that were infected with the *exuR* mutant survived (Fig. 3a). Deletion of *exuR* also affected murine colonization, with decreased *exuR* loads in stools and cecal content compared to mice infected with wild-type (WT) (Fig. 3b,d). The *exuR* failed to colonize the cecal and colonic tissue (Fig. 3c,e). Tissue colonization of *C. rodentium* is strictly dependent on the LEE-encoded T3SS⁴. Congruent with the marked reduction in the transcript levels of LEE-encoded genes *in vitro* (Extended Data Fig. 3b), the transcript levels of LEE-encoded genes *ler*, *espA*, and *tir* in mice infected with the *exuR* mutant was decreased compared to WT (Fig. 3f-h). Pathology and expression of pro-inflammatory cytokines (Nos2 and IL-22) were also decreased in animals infected with *exuR* (Fig. 3 i-l). Histological damage in WT-infected mice was characterized by the presence of edema, the noticeable loss of epithelial integrity, moderate to severe crypt hyperplasia, loss of goblet cells, immune cell infiltration into the lamina propria and submucosa and transepithelial migration of immune cells into the lumen (Fig. 3i,l). In contrast, histopathology scores in mice infected with the *exuR* mutant was comparable to uninfected controls. Taken together, colitis severity corresponded with the decreased ability of the *exuR* mutant to establish a successful infection in the murine colon, and its decreased lethality in comparison to its parental DBS100 strain.

Because ExuR activates expression of the T3SS (Fig.1) that leads to induction of inflammation in the gut³, we investigated whether ExuR was necessary for *C. rodentium* colonization after inflammation occurred. To induce inflammation, we utilized chemical induction of colitis by treatment with dextran sodium sulfate (DSS). DSS directly damages the colonic epithelium and induces severe colitis in the absence of any bacterial pathogen²⁴. DSS treatment sensitized mice to such a degree that they become susceptible to infection by *exuR* (Fig. 4). The *exuR* colonized mice to a similar degree of WT (Fig. 4a), and had higher bacterial loads in the cecum content and tissue of DSS-treated mice compared to non-inflamed animals (Figure 4b,c). Consistent with the fact that DSS treatment rescued tissue colonization; DSS-treated animals succumb to death during a *exuR C. rodentium* infection

(Fig. 4d). Together, these data show that ExuR is not essential for survival in an inflamed gut, and that its principal role is the induction of inflammation by regulating the LEE.

Microbiota-pathogen relationships in the catabolism of sugar acids for intestinal colonization by *C. rodentium rodentium*.

To better understand the role of sugar acid catabolism in *C. rodentium* intestinal colonization, we generated an *uxaC* mutant. In the Ashwell pathway, the *uxaC* gene encodes for an uronate isomerase, which is the first step in the catabolic pathway for galacturonic-acid and glucuronic-acid utilization. UxaC converts galacturonic-acid in tagaturonate that is converted by UxaB into altronate. Glucuronic-acid is converted into fructuronate by UxaC, and fructuronate is converted into mannonate by UxuB (Fig. 5a)^{14,16}. EHEC utilizes both galacturonic and glucuronic-acids as sugar sources, albeit galacturonic-acid enhances EHEC's growth, while its growth is decreased by glucuronic-acid as compared to glucose as the only sugar source²⁵. However, *C. rodentium* was incapable of growing with glucuronic-acid as a sole carbon source, while it grew similar to glucose in galacturonic-acid (Extended Data Fig. 3d). Moreover, while galacturonic-acid decreased LEE gene expression in EHEC, glucuronic-acid had no effect in LEE gene expression (Fig. 2 and Extended Data Fig. 4). In *E. coli*, including EHEC, there is a second regulator, UxuR that acts together with ExuR to regulate expression of the *uxa* and *uxu* genes necessary for the transport and catabolism of sugar acids¹⁴⁻¹⁶. *C. rodentium* only encodes ExuR²⁶. Both *exuR* and *uxuR* were deleted independently and together in EHEC. We only observed decreased LEE expression in *exuR* and not in *uxuR* (Extended Data Fig. 4). Furthermore, double deletion of *exuR* and *uxuR* in EHEC, mimics the phenotype of single *exuR* knockout (Extended Data Fig. 4). Together, these data indicate that LEE regulation by occurs primarily by galacturonic-acid through ExuR.

Deletion of *uxaC* renders EHEC and *C. rodentium* incapable of utilizing galacturonic-acid as a carbon source (Extended Data Fig. 2a). In C3H/HeJ mice the *uxaC* mutant had a significant decrease in colonization up until 2 days post-infection compared to WT infected animals. However, this difference in colonization is no longer observed as infection progresses (Fig. 5b,e). Competition experiments further confirmed these results, with the *uxaC* mutant being outcompeted by WT at day 2 post-infection (Fig. 5c). It is notable that this initial advantage for galacturonic-acid utilization in intestinal colonization is due to its metabolism by *C. rodentium*, and not through differences in LEE expression, as *uxaC* expresses the LEE at similar levels to WT during murine infection (Fig. 5d). These data suggest that catabolism of sugar acids plays a role in initial intestinal expansion by *C. rodentium*, but is not necessary later on during infection (Fig. 5b).

To further probe the role of ExuR regulation of the Ashwell pathway and the LEE during murine infection, we infected mice with WT, *uxaC*, *exuR*, and *uxaC exuR* () mutants, and determined the bacterial burden and survival (Fig. 5e-g). Mice that were infected with the double mutant were not significantly different from the single *exuR* mutant in regards to stool and tissue bacterial loads, pathology scores (Extended Data Fig. 5), as well as survival (Fig. 5e-g). Although the *uxaC* presents decreased stool burdens compared to WT up until 2 days post infection (Fig. 5b,e), it does not have a defect in cecum

tissue colonization, which is a LEE dependent phenotype (Fig. 5f). Moreover, *uxaC* infected animals succumb to death similarly to WT infected animals, and have increased pathology compared to *exuR* and *uxaC exuR* (Fig. 5g and Extended Data Fig. 5). Competition experiments show that WT outcompetes *exuR* and *exuR uxaC* 1,000-fold, while *uxaC* is outcompeted by WT only by 10-fold (Fig. 5h). Indicating that colonization of the gut is mainly accomplished by the activity of the LEE activation through the ExuR transcriptional regulator. Furthermore, the single *uxaC* mutant outcompetes the double *exuR uxaC* mutant, indicating that deletion of *exuR* is detrimental towards colonization even in the absence of sugar acid catabolism (Fig. 5h). UxaC acts on both glucuronic and galacturonic acid. Therefore, changes in murine colonization by *uxaC* is representative of the overall role of sugar acid utilization, without discriminating between the two branches of the Ashwell pathway. To address this, we also independently deleted the *uxaB* and *uxuB* genes in *C. rodentium* and performed further competition experiments *in vivo*. The *uxaB* has a similar defect to *uxaC*, while *uxuB* had no phenotype (Fig. 5 h). Overall, this suggests that galacturonic and not glucuronic-acid provides the initial fitness advantage for *C. rodentium*.

The T3SS induces inflammation in the gut³. In an already inflamed gut (DSS treatment) mice succumb to infection by *exuR* (Fig. 4), and congruent with these data, *exuR* is not outcompeted by WT in these animals (Fig. 5h). However, the *uxaC* is similarly outcompeted by WT in the absence or presence of inflammation (Fig. 5h). Hence, catabolism of sugar acids does not play a significant role in the regulation of the T3SS *in vivo*, indicating that regulation of the T3SS through ExuR is independent of its role in regulation of metabolism of sugar acids. These data suggest that sugar acid utilization plays a role in early pathogen expansion but is not involved in virulence.

In the GI tract the main source of pectin is diet. Pectin is a polysaccharide found in plant cell walls²⁷, which can be digested, releasing galacturonic-acid, by saccharolytic members of the microbiota, such as *Bt*^{28,29}. In the presence of galacturonic-acid, ExuR repression of the genes encoding enzymes involved in its utilization is released^{9,10}, while LEE gene expression is decreased (Fig. 2). Consistent with this regulation, expression of *uxuA* and *uxaC* is only increased in the presence of *Bt* when pectin is present (Fig. 6b,c). Expression of the LEE gene *espA* is decreased in the presence of *Bt* when pectin is present (Fig. 6a). However, *espA* expression is increased in the presence of *Bt* in the absence of pectin (Fig. 6a), due to the production of succinate by *Bt*, as previously described³⁰. *Bt* can harvest several sugars from mucin, and digest pectin releasing galacturonic-acid^{28,29}. Supernatants of *Bt* grown in a defined medium with either mucin or pectin as carbon sources were used in *in vitro* competition experiments between WT and *uxaC* (can't utilize galacturonic-acid as sugar source), to investigate whether galacturonic acid utilization conferred a growth advantage to *C. rodentium* in relation to other sugar sources. The WT outcompeted *uxaC* 10-fold in mucin-pre-conditioned media, while it outcompeted *uxaC* 100-fold in pectin-pre-conditioned media (Fig. 6d). Importantly, there were no differences in the competitive index between WT and *uxaC* under growth on mannan or starch, which are substrates that do not contain uronic acids (Fig. 6d). These data indicate that *Bt* releases galacturonic-acid from pectin increasing expression of the galacturonic acid utilization genes, leading to a growth expansion of *C. rodentium*, while expression of the T3SS is decreased.

To address the role of pectin in *C. rodentium* murine colonization and infection, mice were either fed pectin or not. However, we noticed that C3H/HeJ mice fed pectin presented basal levels of inflammation compared to the mice that were not fed pectin (Extended Data Fig. 6). To avoid these issues we then used C57BL/6 mice (pectin does not promote inflammation in these animals³¹), which also develop colitis and disease upon *C. rodentium* infection, but do not succumb to death⁴. *C. rodentium* loads were similar in the cecum content (a read out from the luminal environment) of both pectin-treated and non-treated animals (Fig. 6e). However, *C. rodentium* loads were decreased in the cecum tissue of animals treated with pectin (Fig. 6f). Attachment to *C. rodentium* to intestinal tissues is a LEE-dependent phenotype, which is congruent with decreased LEE expression by galacturonic-acid. To further dissect the contribution of pectin degradation by *Bt* in *C. rodentium* murine infection, microbiota-depleted mice through antibiotic treatment^{30,32} were monocolonized with *Bt* or *Bt* PUL75 (does not degrade pectin²⁸), treated or not with pectin, and infected with *C. rodentium*. There were no differences of *C. rodentium* loads in cecum content of these animals (Fig. 6g). However, in animals treated with pectin, *C. rodentium* colonization of cecum tissues was decreased only in animals colonized with *Bt* proficient in pectin degradation (Fig. 6h), and this phenotype was dependent on decreased expression of the LEE (Fig. 6i). Consequently, pectin degradation into galacturonic-acid by *Bt* in the GI tract decreases LEE gene expression, and pathogen adherence to intestinal tissues.

Consequently, diet-derived galacturonic-acid released by the microbiota in the lumen, confers an initial growth advantage to *C. rodentium* early intestinal colonization. This is achieved by utilization of galacturonic-acid as a carbon source and the decreased energetic burden of LEE gene expression. However, as infection progresses and carbon sources are depleted, LEE expression is activated leading to tissue attachment, lesion formation and inflammation. This switch is coordinated through ExuR sensing galacturonic-acid.

Discussion

The nutritional requirements that support the colonization of enteric pathogens are not fully characterized¹. Competition for available nutrients imposes a barrier against colonization, a concept termed colonization resistance. Pathogens engage in distinct metabolic strategies from the resident microbiota to avoid competing for similar nutrients^{33–36}. Because of its very small infectious dose (estimated at 50CFUs)³, EHEC has evolved to utilize different nutrient sources than closely related commensals to avoid direct competition. Notably, utilization of sugar acids is required for full colonization of the gut by EHEC, but not by the closely related commensal strains Nissle 1917, and HS¹⁰. AE pathogens such as EHEC and *C. rodentium* also require a T3SS to outcompete the resident microbiota and colonize the large intestine⁵. However, expression of a T3SS also constitutes a considerable metabolic burden for these pathogens, thus requiring exquisite regulation^{13,34,37}. It is noteworthy that the EHEC T3SS has a modified translocon, where the EspA protein forms a sheath around the needle resulting in a structure as large as a flagellum³⁸. This expensive T3SS machinery combined with EHEC's low infectious dose requires regulation by a complex cellular web with intersecting circuits¹³. To coordinate its metabolism and virulence strategies towards successful gut colonization, EHEC utilizes several nutrients as both metabolites and signals.

Ethanolamine, succinate and fucose are used as both nutrients for pathogen expansion and signals to regulate LEE gene expression by EHEC^{30,37,39,40}. The availability of these nutrient/signals is modulated by the resident microbiota, whether they are directly produced or harvested from the host by the microbiota^{13,30,37,39,40}. These studies highlight that some enteric pathogens evolved ways to exploit the microbiota, creating a “collaborative” environment in which they thrive.

Here we show another example of microbiota-pathogen “collaboration”. Galacturonic-acid is a carbon source made available in the gut by saccharolytic members of the microbiota, such as *Bt*, through the digestion of dietary pectin^{27,41} (Figure 6). Galacturonic-acid is used by EHEC and *C. rodentium* in the gut as a carbon source aiding these pathogens’ initial expansion¹⁰ (Fig. 5). Galacturonic-acid is sensed through ExuR, which in the absence of this sugar acid, presumably as infection progresses, acts as a transcriptional activator of the LEE (Figs. 1,2). Importantly this ExuR-galacturonic-acid regulation plays a key role in the establishment and progression of *C. rodentium* murine infection (Figs. 3–5). In this scenario the pathogen’s ability to gauge the concentration of galacturonic-acid, and its ability to moonlight it as a nutrient and a signal plays a key role in its adaptation to the GI environment, and its ability to out-compete the microbiota to find a suitable colonization niche.

The relationships among host, microbiota and enteric pathogens are complex and multi-layered. It involves a high level of integration between metabolic circuits and virulence gene expression. This research is a step forward to define the molecular mechanisms that govern how commensal species impact virulence of an intestinal pathogen. It has fundamental implications for how differential compositions of microbiota may affect disease outcome and susceptibility to pathogens.

Methods

Strains, plasmids, culture conditions.

Strains and plasmids used in this study are listed in Table S1. WT EHEC O157:H7 strain 86–24⁴², *Citrobacter rodentium* (DBS100)⁴³ and their isogenic mutants were routinely grown at 37°C in Luria-Bertani (LB) overnight. *Bacteroides thetaiotaomicron* (B. theta) VPI-5482 was routinely grown anaerobically overnight at 37°C in TYG medium. To express the type III secretion system (T3SS) low glucose (1g/l) Dulbecco eagle medium (DMEM) was used at 37°C as these conditions have been shown to induce the T3SS under microaerobic conditions^{22,25}. Anaerobic growth was performed using either GasPak EZ anaerobe container system (Becton Dickinson) or Bactron EZ anaerobic chamber (Sheldon Manufacturing). For co-culture experiments between *Bacteroides thetaiotaomicron* and EHEC, the strains were grown overnight as described above and later grown anaerobically in low glucose DMEM in a 10:1 ratio (Bacteroides:EHEC) and supplemented with 1% galacturonic acid or citrus-peel pectin from sigma CAS# 9000-69-5.

Recombinant DNA techniques.

All primers used for mutant and plasmid construction can be found in Table S2.

Mice.

Mice were housed under specific pathogen-free conditions and maintained on a 12 hr light/dark cycle with access to food (5053 Rodent diet 20, PicoLab) unless otherwise noted, and water ad libitum. We used 8–12-week-old female C3H/HeJ or C57BL/6 mice that were purchased from Jackson Laboratories. We used female mice to facilitate randomized mixing between the experimental groups before every experiment. Researchers were not blind to the experimental groups and sample size was chosen empirically. Mice were used as hosts for *Citrobacter rodentium* infection studies. All experiments were performed using protocols approved by UT Southwestern's institutional animal care and use committee (IACUC).

Epithelial Cells.

HeLa cells were obtained from ATCC and kept stored liquid nitrogen until used. HeLa cells were not independently authenticated by our laboratory. They were grown in DMEM supplemented with 10% fetal bovine serum (FBS) and 1% penicillin/streptomycin/gentamicin (PSG) antibiotic mix at 37°C, 5% CO₂. They were screened for being free of Mycoplasma by PCR with primers designed to detect Mycoplasma 16S RNA.

Isogenic Mutant Construction.

Construction of EHEC *exuR* and *uxaC* was performed using lambda-red mutagenesis⁴⁴. The primers used to construct mutations are described in Table S2. Briefly, a PCR product was generated using primers containing homologous regions to sequences flanking the *exuR* and *uxaC* genes to amplify a kanamycin resistant gene from pKD4. EHEC 86–24 and *C. rodentium* DBS100 cells harboring pKD46 were electroporated using the PCR product and colonies were selected from kanamycin LB plates. Nonpolar mutants were generated using Flp recombinases encoded in pCP20 plasmid to cleave off the kanamycin cassette. Complementation experiments were conducted using PCR products flanked with restriction enzymes; generated from EHEC 86–24 genomic DNA amplifying *exuR* that was cloned into pACYC184.

RNA extraction and qRT-PCR.

Primers used in qRT-PCR and cloning are listed in Table S2. RNA from 3 biological replicates was extracted using extracted using RiboPure kit according to the manufacturer instructions (Ambion). For *in vitro* experiments, cultures were grown to mid-log (OD₆₀₀ of 0.6) in low glucose-DMEM under microaerobic conditions. RNA was extracted using the RiboPure bacterial isolation kit according to the manufacturer's protocols (Ambion). For *in vivo* experiments, cecal contents were collected from infected mice on day 8 after *C. rodentium* infection, flash frozen in liquid nitrogen and stored at –80°C. The frozen contents were homogenized for two cycles of 45 seconds in a bead beater (BioSpec) and RNA isolated using the RNeasy PowerMicrobiome kit (QIAGEN). The primers used for quantitative reverse transcription-PCR (qRT-PCR) were validated for amplification efficiency and template specificity. Quantitative reverse transcription-PCR (qRT-PCR) was performed as follows. Briefly, 2µg of diluted extracted RNA was converted to cDNA with addition of superscript, random primers, DTT and dNTPs. Validated Primers (Table S2) and SYBR Green were added to the cDNA and the mix run in Quantstudio 6 flex (Applied

Biosystems). Data were collected using QuantStudio Real-Time PCR Software v1.3, normalized to endogenous *rpoA* and *rpoZ* levels, and analyzed using the comparative critical threshold (CT) method. The Student's paired t-test was used to determine statistical significance. A P value of <0.05 was considered significant.

RNA-seq.

Briefly, RNA extracted as described above was used to perform RNA sequencing experiments. RNA isolated from three replicates was sent for RNA sequencing at UT Southwestern medical center Next Generation Sequencing Core. RNA libraries were prepared using Illumina ScriptSeq Complete Kit (Bacteria) (Catalog #BB1224). RNA libraries were run on Illumine HiSeq 2500 sequencer with SE-50. The raw data generated was analyzed using DNASTAR Lasergene software. All experiments were normalized by reads assigned per kilobase of target per million mapped reads (RPKM). RNA seq data can be accessed at European Nucleotide Archive accession number: PRJEB30676.

Fluorescent Actin Staining Assay.

Fluorescein actin staining (FAS) assays were performed as previously described⁴⁵. Briefly, HeLa cells were grown to 80% confluency. The wells were washed with PBS and replaced with low-glucose DMEM supplemented with 10% FBS. Bacterial cultures were grown aerobically overnight as described above at 37°C. Overnight bacterial cultures were diluted 1:100 in low-glucose DMEM and grown for 4 hrs. This culture was used to infect confluent monolayers of HeLa cells for 3 h at 37°C, 5% CO₂. After a 3 hr infection, the coverslips were washed, fixed, permeabilized, and then treated with fluorescein isothiocyanate (FITC)-labeled phalloidin to visualize actin accumulation. The coverslips were mounted on slides and visualized with a Zeiss Axiovert microscope. The number of bacteria attached per HeLa cell was quantified. Replicate coverslips from multiple experiments were quantified, and statistical analyses were performed.

Protein Purification and Electrophoretic Mobility Shift Assay.

ExuR was cloned into the *Nde* I and *Bam*H I sites of pASK-IBA32 by Gibson cloning, Table S2, to create an N-terminal His-tagged construct. This was transformed into BL21 cells. His-tagged ExuR was purified using the AKTA START system with pre-packed nickel columns according to manufacturer's instructions. For EMSA, DNA probes were prepared by PCR from genomic templates. Probes were purified by DNA electrophoresis and agarose gel extraction using a QIAquick Gel Extraction Kit from QIAGEN per the manufacturers instructions. The amplicons were labeled with ³²P γ -ATP by T4 PNK from NEB. Labeled probes were further purified by Qiagen PCR purification kit. EMSA reactions were prepared as follows (50 mM NaKPO₄ pH 7.5, 100 mM NaCl, 1.5 mM DTT, 100 μ g/mL BSA, 250 μ g/mL sonicated salmon sperm DNA) with the indicated protein concentrations. Binding was resolved on 5% polyacrylamide gels in Tris/borate/EDTA. Gels were dried onto filter paper and exposed to phosphorimager screens and assessed on a GE Typhoon scanner.

Western blotting of secreted and lysate fractions.

Secreted proteins were prepared as described previously⁷. In brief, cultures were grown microaerobically in low-glucose DMEM at 37°C and collected at an OD₆₀₀ of 0.6. Total secreted proteins from culture supernatants were separated from bacterial cells using centrifugation and filtration. The proteins were separated by SDS-PAGE and subjected to immunoblotting with rabbit polyclonal antiserum to EspA and EspB and visualized with enhanced chemiluminescence (Bio-Rad). Whole-cell lysates were prepared from strains grown microaerobically in low-glucose DMEM and collected after OD₆₀₀ of 0.6 growth phase. Cells were collected by centrifugation and then lysed with urea lysis buffer (100 mM NaH₂PO₄, 10 mM Tris, 8 M urea, pH 6.3). Samples were probed using antisera against EspA, EspB, and Tir.

In vitro competition experiments.

Bacteroides thetaiotaomicron was anaerobically grown for 48 hours in minimal medium containing 100 mM KH₂PO₄ (pH 7.2), 15 mM NaCl, 8.5 mM (NH₄)₂SO₄, 4 mM L-cysteine, 1.9 μM hematin/200 μM L-histidine 100 μM MgCl₂, 1.4 μM FeSO₄•7H₂O, 50 μM CaCl₂, 1 μg ml⁻¹ vitamin K3, and 5 ng ml⁻¹ vitamin B12. Mucin and pectin were added to MM at a final concentration of 1%. Media were filter sterilized using a Millipore Express filter unit (0.22 μm pore diameter). The culture was centrifuged at 3,900 RPM for 15 minutes and the supernatant was collected and filtered through a 0.22 μm filter. Supernatants were inoculated with a 1:1 ratio of *C. rodentium* and the competitive index was determined 24 hours post-inoculum by plating on selective agar plates.

Citrobacter rodentium infection.

C. rodentium was grown overnight in Luria-Bertani (LB) broth supplemented with nalidixic acid (NalA, 30 μg/ml) with shaking at 37°C. Mice were infected by oral gavage with 100 μL of PBS containing approximately 1 × 10⁹ CFU of *C. rodentium*. To determine the bacterial numbers in the feces, fecal pellets were collected from individual mice, weighed, and homogenized in cold PBS and plated at serial dilutions onto LB agar containing 30 μg/ml NalA, and the number of CFU was determined after overnight incubation at 37°C. Mice were sacrificed at various time points post-infection. The cecum content and tissue were collected to determine the amount of CFU and RT-qPCR analysis. The cecal patch were fixed in 10% formalin and then processed for H&E staining. In competitive infections, a 1:1 ratio of two *C. rodentium* strains were given via oral gavage at a combined final concentration of 1 × 10⁹ CFU/mouse. Cecal contents were collected 2 days post-infection and placed into sterile PBS and were serially diluted on selective agar plates to determine CFU/g of each strain. The competitive indices were calculated by dividing the CFU/g of wild-type *C. rodentium* recovered over the CFU/g of mutant recovered, and later normalized to the same ratio in the inoculum. For the pectin diet experiments we used 8–12 week-old female C57Bl/6 mice that were purchased from Jackson Laboratories. From arrival the mice were switched to a control diet TD.94096 (Casein 200.0, DL-Methionine 3.0, Sucrose 494.787, Corn Starch 150.0, Corn Oil 50.0, Cellulose 50.0, Mineral Mix AIN-76 35.0, Vitamin Mix AIN-76A 15.0, Choline Bitartrate 2.2, Vitamin K, MSB complex 0.003 Ethoxyquin, antioxidant 0.01) or a 5% citrus-peel pectin (CAS# 9000-69-5) diet TD.170515 (Casein

200.0, DL-Methionine 3.0, Sucrose 494.787, Corn Starch 150.0, Corn Oil 50.0, Pectin 50.0, Mineral Mix AIN-76 35.0, Vitamin Mix AIN-76A 15.0, Choline Bitartrate 2.2, Vitamin K, MSB complex 0.003 Ethoxyquin, antioxidant 0.01) from Envigo. These mice were cleared of their intestinal microbiota by a daily gavage of four antibiotics: ampicillin, neomycin, metronidazole, and vancomycin (5 mg of each antibiotic per mouse per day) for 3 days^{30,32}. Fecal pellets were collected before and after antibiotic treatment to confirm depletion of the gut microbiota. Briefly, the feces were resuspended in PBS and plated on brain heart infusion (BHI)-blood agar plates containing no antibiotics. Colony counts were performed after 48-h incubation at 37°C under both aerobic and anaerobic conditions. Following antibiotic depletion the mice were orally gaged with 3×10^9 CFU of *Bacteroides thetaiotaomicron* (*B. theta*) VPI-5482 or the PUL75 deletion mutant (non-pectin degrader). The following day the mice were infected with *C. rodentium* and the experiment followed as described above.

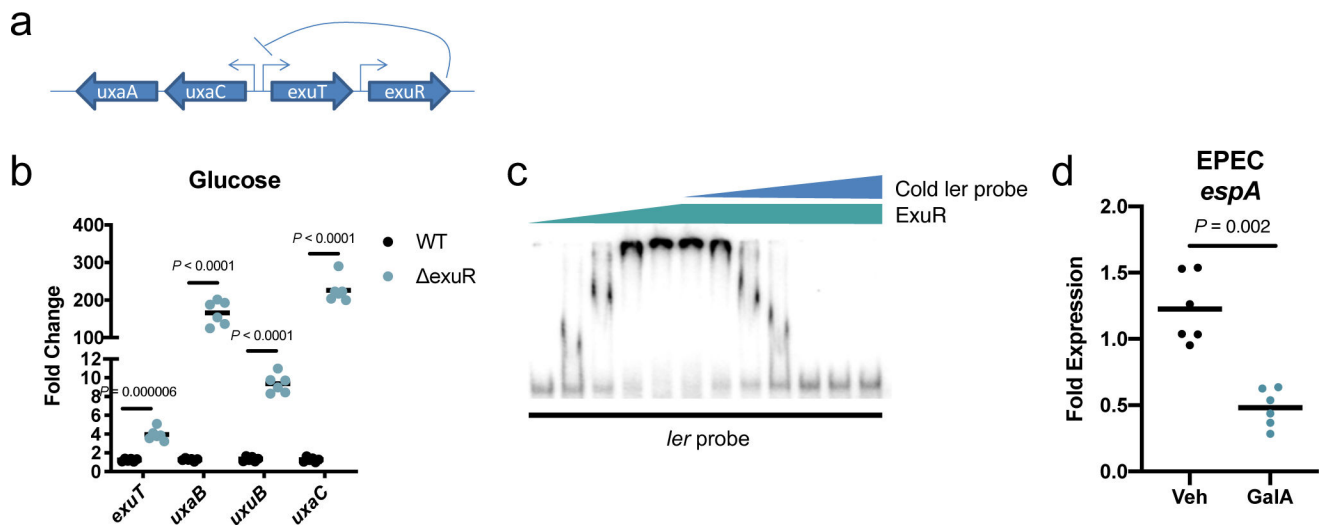
Histopathology.

At necropsy, cecum and colon segments were fixed in 10% neutral buffered formalin. Hematoxylin and eosin stained sections were blindly scored for inflammation severity. Briefly, inflammation was assessed based on the following histopathological features: submucosal edema (0–4), goblet cell depletion (0–4), epithelial hyperplasia (0–4), epithelial integrity (0–4), polymononuclear (PMN) cell and inflammatory monocyte infiltration (0–4) and bacterial epithelial attachment (0–3). Data are expressed as the sum of these individual scores (0–23).

Data availability.

The data that support the findings of this study are available from the corresponding author upon request.

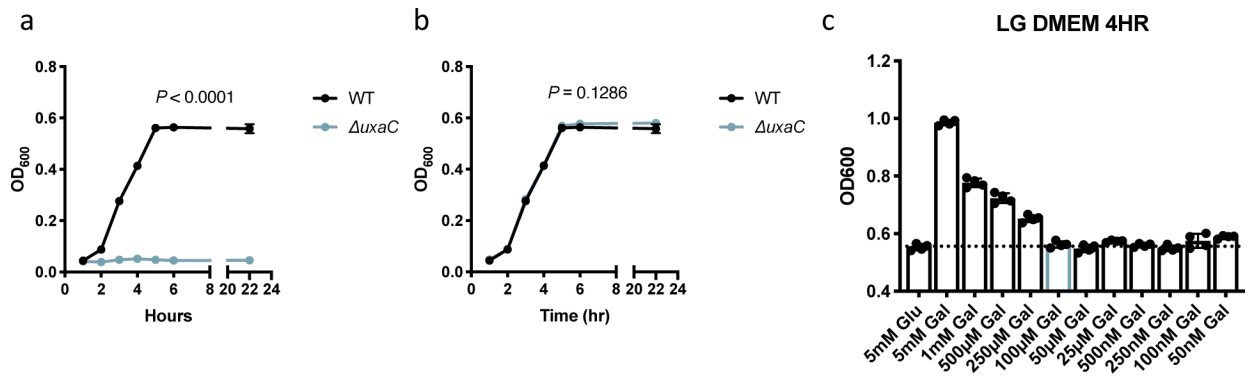
Extended Data



Extended Data 1]. ExuR regulates genes encoding enzymes necessary for the catabolism of galacturonic-acid.

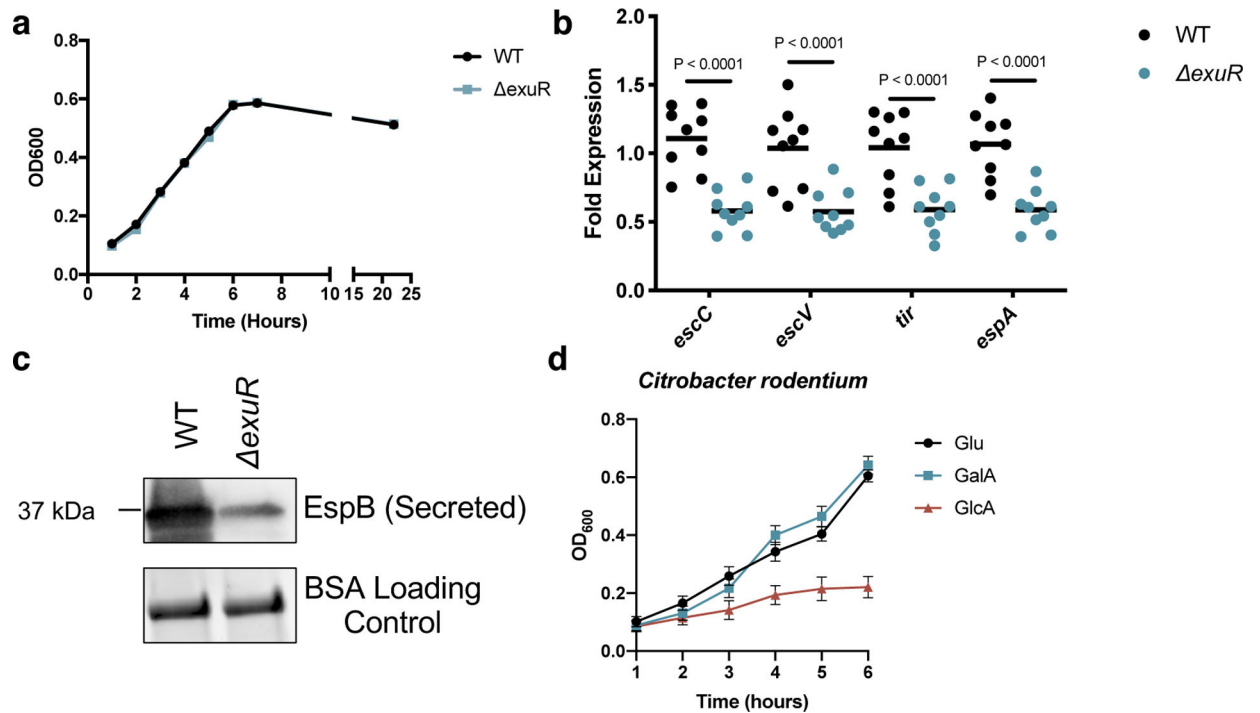
a. Schematic representation of ExuR repression of the galacturonic-acid utilization genes. **b.** qRT-PCR of the galacturonic utilization genes in WT ($n = 3$) and $\Delta exuR$ ($n = 3$) EHEC (n , number of biological replicates; results are representative of two independent experiments). The mean and P value for two-sided Mann-Whitney statistical analysis are shown. **c.** Competition EMSA of ExuR binding to the *ler* promoter in the absence and presence of *ler* cold probe. Results are representative of two independent experiments with similar results. **d.** qRT-PCR of the LEE *espA* gene in EPEC in the presence of vehicle ($n = 6$) or galacturonic-acid (GalA) ($n = 6$) (n , number of biological replicates; results are representative of two independent experiments). The mean and P value for two-sided Mann-Whitney statistical analysis are shown.

(n , number of biological replicates; results are representative of one independent experiments). The mean and P value for two-sided Mann-Whitney statistical analysis are shown.



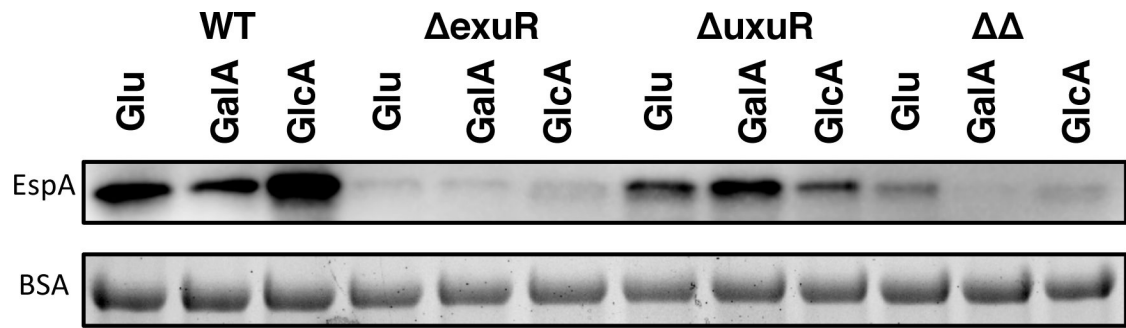
Extended Data 2]. UxaC and galacturonic acid promotion of EHEC's growth.

a, Growth curves of WT ($n = 2$) and *uxaC* ($n = 2$) EHEC in M9 minimal medium with 5mM galacturonic-acid as a sole carbon source (n , number of biological replicates; results are representative of one independent experiments). The mean \pm SD and P value for two-sided two-way ANOVA statistical analysis are shown. **b**, Growth curves of WT ($n = 4$) and *uxaC* ($n = 4$) EHEC in low glucose DMEM (n , number of biological replicates; results are representative of one independent experiments). The mean and P value for two-sided one-way ANOVA statistical analysis are shown. **c**, Growth of WT EHEC in low glucose DMEM supplemented with different concentrations of galacturonic acid.



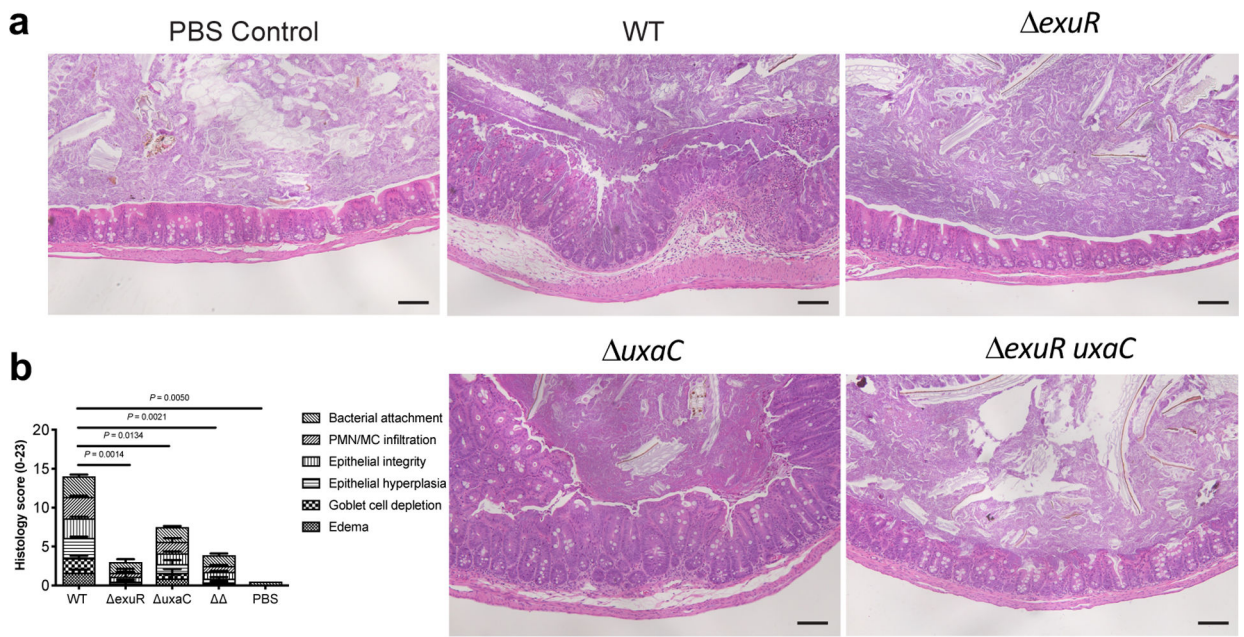
Extended Data 3]. ExuR also activates the LEE in *C. rodentium*.

a. Growth curve of WT ($n = 3$) and $exuR$ ($n = 3$) *C. rodentium* strains grown in low-glucose DMEM under microaerobic conditions (n , number of biological replicates; results are representative of one independent experiments). The mean \pm SD value for two-sided one-way ANOVA statistical analysis are shown. **b.** RT-qPCR of the LEE-encoded genes in *escC*, *escV*, *tir*, and *espA* in WT ($n = 9$) and $exuR$ ($n = 9$) *C. rodentium* (n , number of biological replicates; results are representative of three independent experiments). The mean and P value for two-sided two-way ANOVA statistical analysis are shown. **c.** Western blot for secreted EspB in WT and $exuR$ *C. rodentium*. Representative blots from three independent experiments. **d.** Growth curves of *C. rodentium* with glucose (Glu) ($n = 3$), galacturonic acid (GalA) ($n = 3$) or glucuronic acid (GlcA) ($n = 3$) as sole carbon sources (n , number of biological replicates; results are representative of three independent experiments). The mean \pm SD value for two-sided one-way ANOVA statistical analysis are shown.



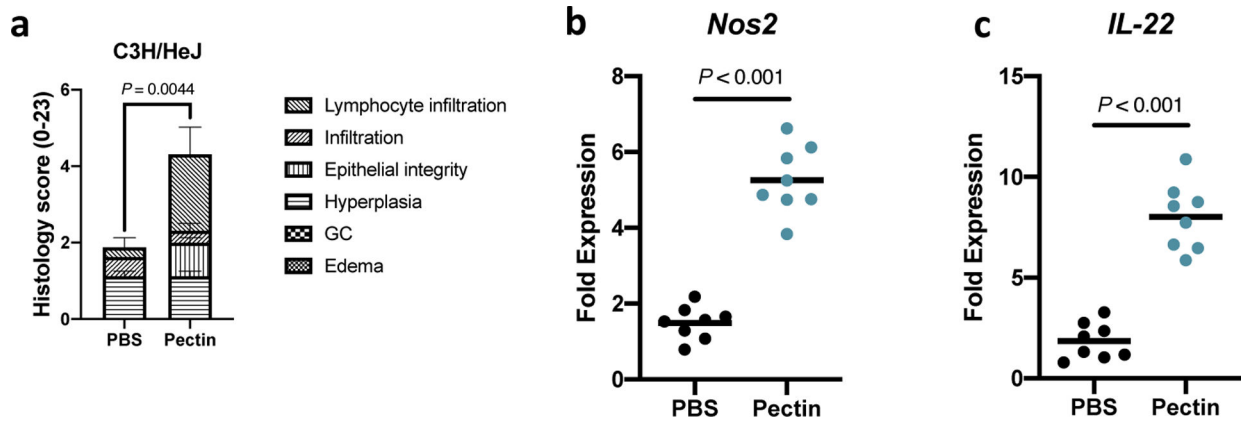
Extended Data 4]. Galacturonic-acid acts through ExuR to decrease LEE gene expression.

Western blot of supernatants from EHEC WT, *exuR*, *uxuR* and *exuRuxuR* () grown in the presence of glucose (Glu), galacturonic-acid (GalA), or glucuronic acid (GlcA) in DMEM probed with anti-EspA antiserum. BSA is used as a loading control. Representative blots from three independent experiments.



Extended Data 5]. Mice infected with *uxaC* *C. rodentium* have only a mild increase in inflammation.

C3H/HeJ mice under non-infected conditions as well as at post-infection day 8 with WT or the *exuR*, *uxaC* and *exuR uxaC* mutants. **a**, Hematoxylin-eosin-stained cecal patch tissues of C3H/HeJ mice. Representative images from two independent experiments, scale bars = 100 μ m. **b**, Blinded histopathology scores of non-infected mice or infected with WT ($n = 4$) or the *exuR* ($n = 4$), *uxaC* ($n = 4$), and *exuR uxaC* ($n = 4$) *C. rodentium* (n , number of biological replicates; results are representative of two independent experiments). The mean and P value for two-sided one-way ANOVA statistical analysis.



Extended Data 6]. Pectin engenders inflammation in C3H/HeJ mice.

C3H/HeJ mice were treated with 200 μ L of 2% pectin or PBS. **a**, Blinded histopathology scores of non-infected mice treated with 200 μ L of 2% pectin ($n = 4$) or PBS ($n = 4$) (n , number of biological replicates; results are representative of two independent experiments). The mean and P value for two-sided one-way ANOVA statistical analysis. **b-c**, RT-qPCR determined the expression of *Nos2* and *IL22* genes in the cecal tissue of mice treated with 200 μ L of 2% pectin ($n = 4$) or PBS ($n = 4$) (n , number of biological replicates; results are representative of two independent experiments). The mean and P value for two-sided Mann-Whitney statistical analysis are shown. GAPDH was used to normalize gene expression.

Supplementary Material

Refer to Web version on PubMed Central for supplementary material.

Acknowledgements

This study was supported by the NIH grants: AI053067, AI05135, AI077613, AI114511 to VS. AGJ was supported through NIH Training Grant 5 T32 AI7520.

References

1. Sonnenburg JL et al. Glycan Foraging in Vivo by an Intestine-Adapted Bacterial Symbiont. *Science* (New York, N.Y.) 307, 1955(2005).
2. Baumler AJ & Sperandio V Interactions between the microbiota and pathogenic bacteria in the gut. *Nature* 535, 85–93, doi:10.1038/nature18849 (2016). [PubMed: 27383983]
3. Kaper JB, Nataro JP & Mobley HL Pathogenic *Escherichia coli*. *Nat Rev Microbiol* 2, 123–140 (2004). [PubMed: 15040260]
4. Luperchio SA & Schauer DB Molecular pathogenesis of *Citrobacter rodentium* and transmissible murine colonic hyperplasia. *Microbes Infect* 3, 333–340 (2001). [PubMed: 11334751]
5. Kamada N et al. Regulated Virulence Controls the Ability of a Pathogen to Compete with the Gut Microbiota. *Science* (New York, N.Y.) 336, 1325(2012).
6. Slater SL, Sagfors AM, Pollard DJ, Ruano-Gallego D & Frankel G The Type III Secretion System of Pathogenic *Escherichia coli*. *Curr Top Microbiol Immunol* 416, 51–72, doi: 10.1007/82_2018_116 (2018). [PubMed: 30088147]
7. Jarvis KG et al. Enteropathogenic *Escherichia coli* contains a putative type III secretion system necessary for the export of proteins involved in attaching and effacing lesion formation. *Proc Natl Acad Sci U S A* 92, 7996–8000 (1995). [PubMed: 7644527]

8. McDaniel TK, Jarvis KG, Donnenberg MS & Kaper JB A genetic locus of enterocyte effacement conserved among diverse enterobacterial pathogens. *Proc Natl Acad Sci U S A* 92, 1664–1668 (1995). [PubMed: 7878036]
9. Chang D-E et al. Carbon nutrition of *Escherichia coli* in the mouse intestine. *Proceedings of the National Academy of Sciences of the United States of America* 101, 7427(2004). [PubMed: 15123798]
10. Fabich AJ et al. Comparison of carbon nutrition for pathogenic and commensal *Escherichia coli* strains in the mouse intestine. *Infect Immun* 76, 1143–1152, doi:IAI.01386–07 [pii] 10.1128/IAI.01386-07 (2008). [PubMed: 18180286]
11. Maltby R, Leatham-Jensen MP, Gibson T, Cohen PS & Conway T Nutritional basis for colonization resistance by human commensal *Escherichia coli* strains HS and Nissle 1917 against *E. coli* O157:H7 in the mouse intestine. *PLoS One* 8, e53957, doi:10.1371/journal.pone.0053957 (2013). [PubMed: 23349773]
12. Peekhaus N & Conway T What’s for dinner?: Entner-Doudoroff metabolism in *Escherichia coli*. *Journal of bacteriology* 180, 3495–3502 (1998). [PubMed: 9657988]
13. Pifer R, Russell RM, Kumar A, Curtis MM & Sperandio V Redox, amino acid, and fatty acid metabolism intersect with bacterial virulence in the gut. *Proceedings of the National Academy of Sciences of the United States of America* 115, E10712–E10719, doi:10.1073/pnas.1813451115 (2018). [PubMed: 30348782]
14. Robert-Baudouy J, Portalier R & Stoeber F Regulation of hexuronate system genes in *Escherichia coli* K-12: multiple regulation of the *uxu* operon by *exuR* and *uxuR* gene products. *J Bacteriol* 145, 211–220 (1981). [PubMed: 7007313]
15. Blanco C, Ritzenthaler P & Kolb A The regulatory region of the *uxuAB* operon in *Escherichia coli* K12. *Molecular & general genetics* : MGG 202, 112–119 (1986). [PubMed: 3083215]
16. Ritzenthaler P, Blanco C & Mata-Gilsinger M Genetic analysis of *uxuR* and *exuR* genes: evidence for *ExuR* and *UxuR* monomer repressors interactions. *Mol Gen Genet* 199, 507–511 (1985). [PubMed: 3929016]
17. Rodionov DA, Mironov AA, Rakhmaninova AB & Gelfand MS Transcriptional regulation of transport and utilization systems for hexuronides, hexuronates and hexonates in gamma purple bacteria. *Molecular microbiology* 38, 673–683 (2000). [PubMed: 11115104]
18. Suvorova IA et al. Comparative genomic analysis of the hexuronate metabolism genes and their regulation in gammaproteobacteria. *J Bacteriol* 193, 3956–3963, doi:10.1128/JB.00277-11 (2011). [PubMed: 21622752]
19. Tutukina MN, Potapova AV, Cole JA & Ozoline ON Control of hexuronate metabolism in *Escherichia coli* by the two interdependent regulators, *ExuR* and *UxuR*: derepression by heterodimer formation. *Microbiology (Reading, England)* 162, 1220–1231, doi:doi:10.1099/mic.0.000297 (2016).
20. Mellies JL, Elliott SJ, Sperandio V, Donnenberg MS & Kaper JB The Per regulon of enteropathogenic *Escherichia coli* : identification of a regulatory cascade and a novel transcriptional activator, the locus of enterocyte effacement (LEE)-encoded regulator (Ler). *Mol Microbiol* 33, 296–306, doi:1473 [pii] (1999). [PubMed: 10411746]
21. Sperandio V, Mellies JL, Nguyen W, Shin S & Kaper JB Quorum sensing controls expression of the type III secretion gene transcription and protein secretion in enterohemorrhagic and enteropathogenic *Escherichia coli*. *Proc Natl Acad Sci U S A* 96, 15196–15201 (1999). [PubMed: 10611361]
22. Njoroge JW, Nguyen Y, Curtis MM, Moreira CG & Sperandio V Virulence meets metabolism: *Cra* and *KdpE* gene regulation in enterohemorrhagic *Escherichia coli*. *MBio* 3, e00280–00212, doi: 10.1128/mBio.00280-12 (2012). [PubMed: 23073764]
23. Borenshtein D, Nambiar PR, Groff EB, Fox JG & Schauer DB Development of fatal colitis in FVB mice infected with *Citrobacter rodentium*. *Infection and immunity* 75, 3271–3281, doi:IAI.01810–06 [pii] 10.1128/IAI.01810-06 (2007). [PubMed: 17470543]
24. Winter SE et al. Host-derived nitrate boosts growth of *E. coli* in the inflamed gut. *Science* 339, 708–711, doi:10.1126/science.1232467 (2013). [PubMed: 23393266]

25. Carlson-Banning KM & Sperandio V Catabolite and Oxygen Regulation of Enterohemorrhagic *Escherichia coli* Virulence. *MBio* 7, doi:10.1128/mBio.01852-16 (2016).
26. Mundy R, MacDonald TT, Dougan G, Frankel G & Wiles S *Citrobacter rodentium* of mice and man. *Cellular microbiology* 7, 1697–1706, doi:CMI625 [pii] 10.1111/j.1462-5822.2005.00625.x (2005). [PubMed: 16309456]
27. Mohnen D Pectin structure and biosynthesis. *Current opinion in plant biology* 11, 266–277, doi: 10.1016/j.pbi.2008.03.006 (2008). [PubMed: 18486536]
28. Luis AS et al. Dietary pectic glycans are degraded by coordinated enzyme pathways in human colonic *Bacteroides*. *Nature microbiology* 3, 210–219, doi:10.1038/s41564-017-0079-1 (2018).
29. Ndeh D et al. Complex pectin metabolism by gut bacteria reveals novel catalytic functions. *Nature* 544, 65–70, doi:10.1038/nature21725 (2017). [PubMed: 28329766]
30. Curtis MM et al. The gut commensal *Bacteroides thetaiotaomicron* exacerbates enteric infection through modification of the metabolic landscape. *Cell host & microbe* 16, 759–769, doi:10.1016/j.chom.2014.11.005 (2014). [PubMed: 25498343]
31. Umar S, Morris AP, Kourouma F & Sellin JH Dietary pectin and calcium inhibit colonic proliferation in vivo by differing mechanisms. *Cell proliferation* 36, 361–375, doi:10.1046/j.1365-2184.2003.00291.x (2003). [PubMed: 14710853]
32. Kuss SK et al. Intestinal microbiota promote enteric virus replication and systemic pathogenesis. *Science* 334, 249–252, doi:10.1126/science.1211057 (2011). [PubMed: 21998395]
33. Sassone-Corsi M & Raffatellu M No vacancy: how beneficial microbes cooperate with immunity to provide colonization resistance to pathogens. *J Immunol* 194, 4081–4087, doi:10.4049/jimmunol.1403169 (2015). [PubMed: 25888704]
34. Cameron EA & Sperandio V Frenemies: Signaling and Nutritional Integration in Pathogen-Microbiota-Host Interactions. *Cell host & microbe* 18, 275–284, doi:10.1016/j.chom.2015.08.007 (2015). [PubMed: 26355214]
35. Pacheco AR & Sperandio V Enteric Pathogens Exploit the Microbiota-generated Nutritional Environment of the Gut. *Microbiology spectrum* 3, doi:10.1128/microbiolspec.MBP-0001-2014 (2015).
36. Bohnhoff M, Drake BL & Miller CP Effect of streptomycin on susceptibility of intestinal tract to experimental *Salmonella* infection. *Proc Soc Exp Biol Med* 86, 132–137 (1954). [PubMed: 13177610]
37. Pacheco AR et al. Fucose sensing regulates bacterial intestinal colonization. *Nature* 492, 113–117, doi:nature11623 [pii] 10.1038/nature11623 (2012). [PubMed: 23160491]
38. Knutton S et al. A novel EspA-associated surface organelle of enteropathogenic *Escherichia coli* involved in protein translocation into epithelial cells. *The EMBO journal* 17, 2166–2176, doi: 10.1093/emboj/17.8.2166 (1998). [PubMed: 9545230]
39. Kendall MM, Gruber CC, Parker CT & Sperandio V Ethanolamine controls expression of genes encoding components involved in interkingdom signaling and virulence in enterohemorrhagic *Escherichia coli* O157:H7. *MBio* 3, doi:10.1128/mBio.00050-12 (2012).
40. Gonyar LA & Kendall MM Ethanolamine and choline promote expression of putative and characterized fimbriae in enterohemorrhagic *Escherichia coli* O157:H7. *Infect Immun* 82, 193–201, doi:10.1128/IAI.00980-13 (2014). [PubMed: 24126525]
41. Porter NT, Luis AS & Martens EC *Bacteroides thetaiotaomicron*. *Trends Microbiol* 26, 966–967, doi:10.1016/j.tim.2018.08.005 (2018). [PubMed: 30193959]
42. Griffin PM et al. Illnesses associated with *Escherichia coli* O157:H7 infections. A broad clinical spectrum. *Ann Intern Med* 109, 705–712 (1988). [PubMed: 3056169]
43. Barthold SW, Coleman GL, Bhatt PN, Osbaldiston GW & Jonas AM The etiology of transmissible murine colonic hyperplasia. *Lab Anim Sci* 26, 889–894 (1976). [PubMed: 1018473]
44. Datsenko KA & Wanner BL One-step inactivation of chromosomal genes in *Escherichia coli* K-12 using PCR products. *Proceedings of the National Academy of Sciences of the United States of America* 97, 6640–6645, doi:10.1073/pnas.120163297 120163297 [pii] (2000). [PubMed: 10829079]
45. Knutton S, Baldwin T, Williams PH & McNeish AS Actin accumulation at sites of bacterial adhesion to tissue culture cells: basis of a new diagnostic test for enteropathogenic and

enterohemorrhagic *Escherichia coli*. *Infection and immunity* 57, 1290–1298 (1989). [PubMed: 2647635]

Author Manuscript

Author Manuscript

Author Manuscript

Author Manuscript

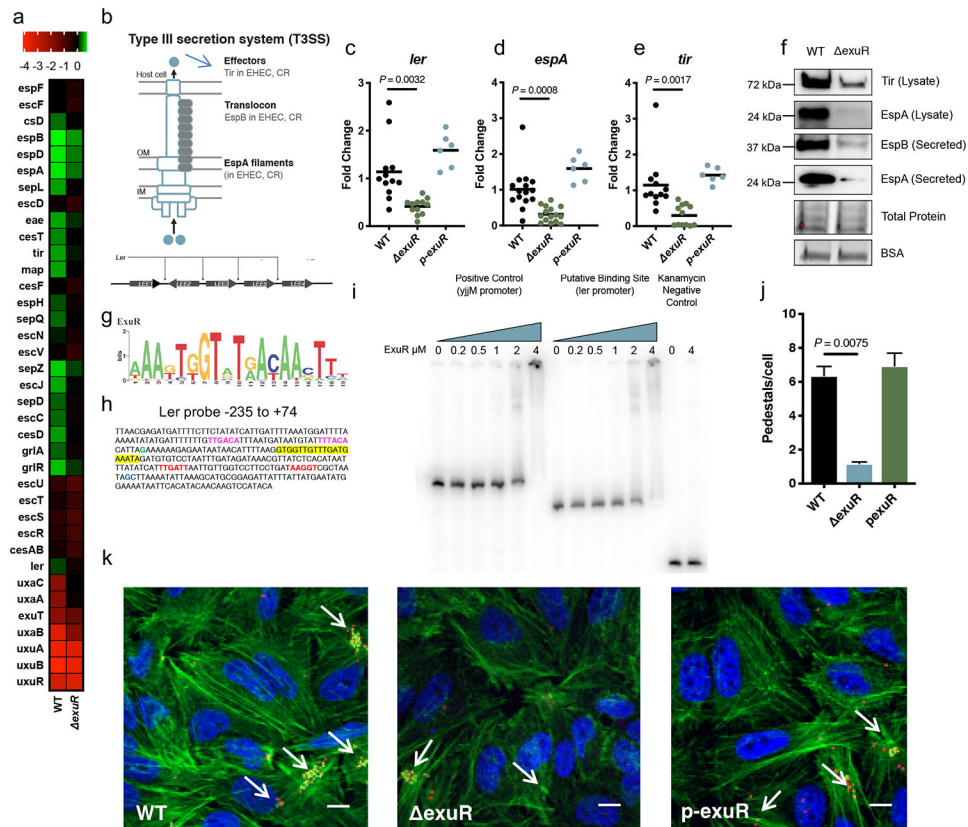


Fig. 1]. ExuR activates expression of the LEE in EHEC.

a, Heat map depicting the top changed transcripts between WT and *exuR* EHEC. **b**, Schematic representation of the LEE-encoded type three secretion system and the LEE island. **c-e**, RT-qPCR for LEE-encoded genes *ler* (**c**), *eae* (**d**), and *espA* (**e**) in WT ($n = 12$), *exuR* ($n = 12$) and complemented (*p-exuR*) ($n = 6$) (n , number of biological replicates; results are representative of three independent experiments). Fold change were calculated relative to *rpoA* as an internal control. The mean and P value for two-sided unpaired Mann-Whitney statistical test are shown. **f**, Western Blot for LEE-encoded proteins Tir, EspB and EspA from secreted and lysate fractions. Total proteins are the loading control for whole cell lysates. Cells were harvested in late logarithmic phase at the same OD₆₀₀, and supernatants were concentrated for secreted proteins. BSA is used as a loading control to ensure there is no variability in the concentration step. Representative blots from three independent experiments. **g**, ExuR consensus sequence. **h**, Sequence of the *ler* probe used for EMSAs depicting the location of the ExuR consensus sequence (highlighted in yellow), promoters P1 (red) and P2 (pink). **i**, EMSA assay for the *ler* putative ExuR binding site, a known target of ExuR, and the kanamycin probe as a negative control. Results are representative of three independent experiments. **j**, Fluorescein actin staining analysis. HeLa cells were infected with mCherry-expressing WT ($n = 100$), *exuR* ($n = 100$) and complemented (*p-exuR*) ($n = 100$) strains of EHEC (n , number of infected HeLa cells enumerated for number of pedestals; results are representative of three independent experiments). Data are represented as the mean \pm SD from three independent experiments. P values were determined by one-way ANOVA statistical analysis. **k**, Representative confocal microscopy images of pedestal

formation (white arrows) by m-Cherry expressing EHEC. DNA (blue) is stained with DAPI and actin (green) is stained with FITC-phalloidin. Images at 40X, scale bar = 20 μ m.

Author Manuscript

Author Manuscript

Author Manuscript

Author Manuscript

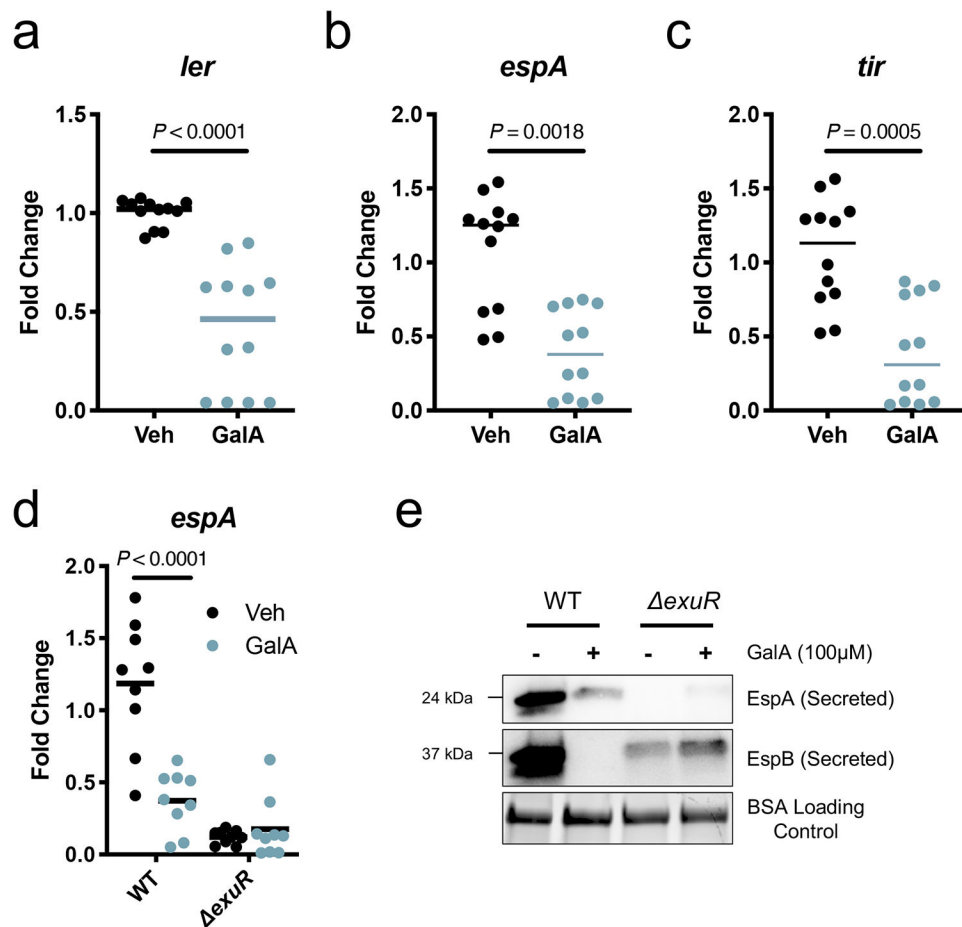


Figure 2]. Galacturonic-acid decreases LEE gene expression.

a-c, RT-qPCR for LEE-encoded genes *ler* (a), *espA* (b), and *tir* (c) in WT ($n = 12$) in the absence (Veh: vehicle) and presence of 100 μM galacturonic-acid (GalA) ($n = 12$). Strains grown in microaerobic conditions at 37°C in DMEM. Data are representative of two independent experiments. Fold change were calculated relative to *irpA* as an internal control. The mean and P value for two-sided unpaired Mann-Whitney statistical test are shown. **d,** RT-qPCR for *espA* from WT ($n = 9$), *exuR* ($n = 9$) EHEC in response to 100 μM galacturonic-acid. Strains grown in microaerobic conditions at 37°C in DMEM. Data are representative of three independent experiments with three biological replicates and three technical replicates. Fold change were calculated relative to *irpA* as an internal control. The mean and P value for two-sided unpaired Mann-Whitney statistical test are shown. **e,** Western Blot for LEE-encoded proteins in wild-type and the *exuR* mutant in response to 100 μM GalA. From secreted and lysate fractions of EHEC grown under microaerobic conditions in DMEM. Total proteins are the loading control for whole cell lysates. Cells were harvested in late logarithmic phase at the same OD_{600} (same number of bacterial cells), and supernatants were concentrated for secreted proteins. Bovine serum albumin (BSA) is used as a loading control to ensure the no variability in the concentration step. Representative blots from three independent experiments.

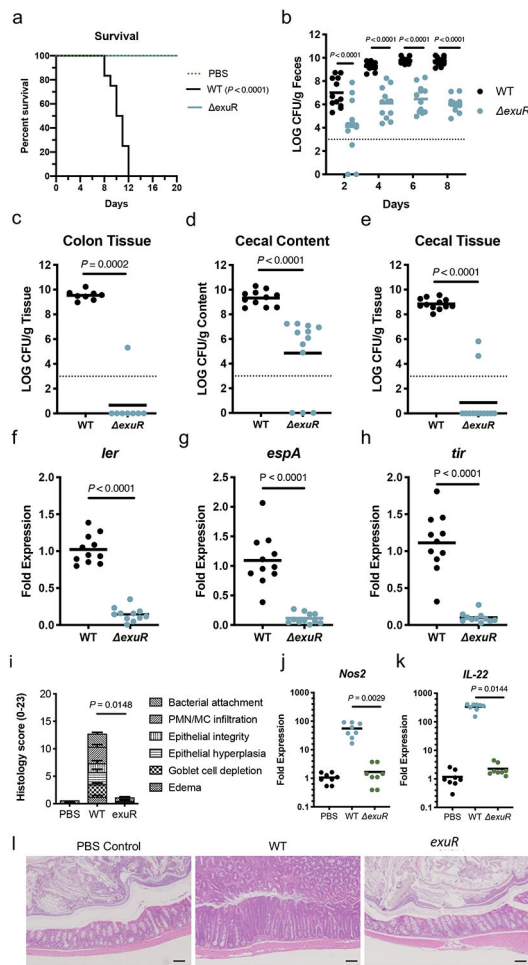


Figure 3]. Deletion of *exuR* results in decreased morbidity and colonization during murine infection by *C. rodentium*.

a. Survival curves from C3H/HeJ mice infected with wild-type (WT, $n = 12$) or *exuR* ($n = 12$) *C. rodentium*. PBS ($n = 8$) was used as a negative control. Statistical significance was calculated using a two-sided log rank (Mantel-Cox) test and P value shown. **b.** Measurement of bacterial CFU from stools of C3H/HeJ mice infected with WT ($n = 12$) or *exuR* ($n = 12$) *C. rodentium*. **c-e.** Measurement of bacterial CFU from C3H/HeJ mice infected with wild-type (WT, $n = 12$) or *exuR* ($n = 12$) *C. rodentium* to assess bacterial abundance from the lumen and epithelium in the cecum and colon at day 8 post-infection (peak of disease). **(c)** *C. rodentium* CFU from cecal content. **(d)** *C. rodentium* CFU from the cecal tissue. **(e)** *C. rodentium* CFU from colon tissue. **b-e.** (n , number of biological replicates; results are representative of three independent experiments). The mean and P value for two-sided unpaired Mann-Whitney statistical test are shown. **f-h.** RT-qPCR for LEE-encoded genes *ler* (**f**), *espA* (**g**), and *tir* (**h**) from the cecal content of mice infected with WT ($n = 8$) or *exuR* ($n = 8$) collected 8 days post infection (n , number of biological replicates; results are representative of two independent experiments). The mean and P value for two-sided unpaired Mann-Whitney statistical test are shown. **i.** Blinded histopathology scores of non-infected mice or infected with WT ($n = 8$) or *exuR* ($n = 8$) *C. rodentium* (n , number of biological replicates; results are representative of two independent experiments). The mean

and *P* value for two-sided one-way ANOVA statistical analysis. **j-k**, RT-qPCR determined the expression of *Nos2* and *IL22* genes in the cecal tissue of C3H/HeJ mice after infection with WT ($n = 8$) or *exuR* ($n = 8$) *C. rodentium* (n , number of biological replicates; results are representative of two independent experiments). The mean and *P* value for two-sided unpaired Kruskal-Wallis statistical test are shown. GAPDH was used to normalize gene expression **l**, Hematoxylin-eosin-stained colon tissues of C3H/HeJ non-infected mice or infected with WT or *exuR C. rodentium* at day 8 post-infection. Representative images from two independent experiments, scale bars = 100 μm .

Author Manuscript

Author Manuscript

Author Manuscript

Author Manuscript

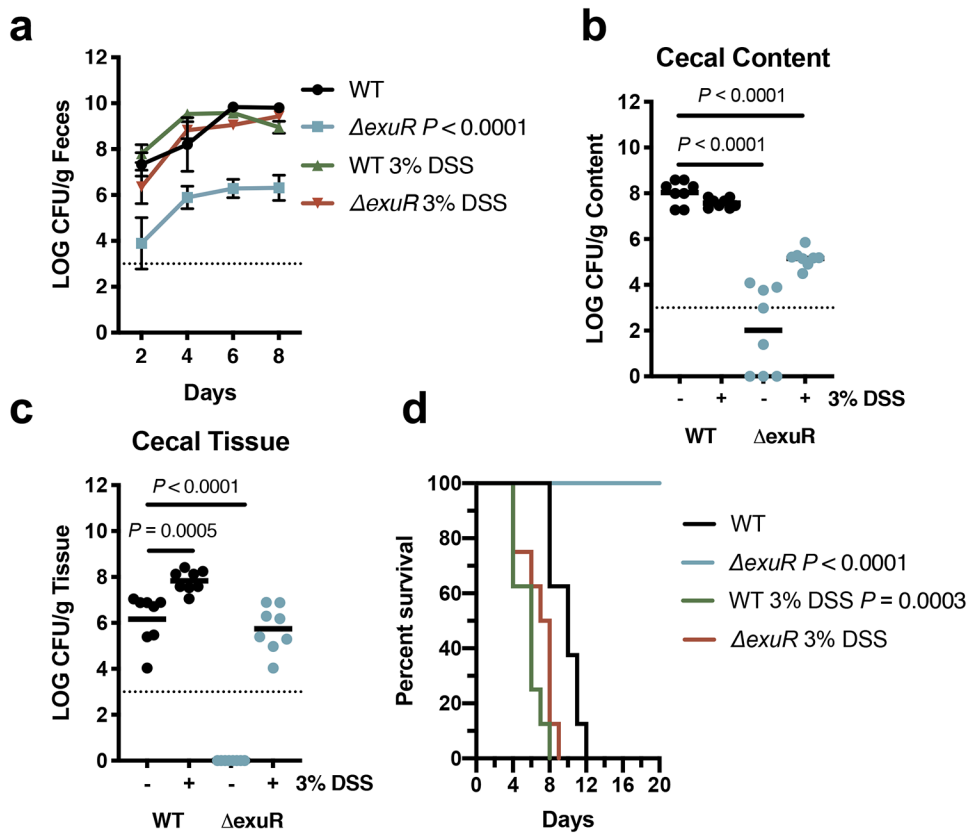


Figure 4]. Chemically induced colitis via DSS treatment rescues colonization and pathogenesis of the *exuR* mutant.

C3H/HeJ mice were treated or not with 3% DSS in their drinking water and allowed to consume ad libitum for 4 days before infection with WT or *exuR* *C. rodentium*. **a**, Measurement of bacterial CFU from stools of non-treated and DSS treated mice infected with WT ($n = 8$) or *exuR* ($n = 8$) *C. rodentium* (n , number of biological replicates; results are representative of two independent experiments). The mean \pm SD and P value for two-sided two-way ANOVA statistical analysis. **b**, *C. rodentium* CFU from the cecal content 8 days post infection (peak of disease) of non-treated and DSS treated mice infected with WT ($n = 8$) or *exuR* ($n = 8$) *C. rodentium*. (n , number of biological replicates; results are representative of two independent experiments). The mean and P value for two-sided two-way Kruskal-Wallis statistical analysis. **c**, *C. rodentium* CFU from the cecal tissue 8 days post infection (peak of disease) of non-treated and DSS treated mice infected with WT or *exuR* *C. rodentium*. $N=8$ per group *** $P < 0.002$, **** $P < 0.0002$, Kruskal-Wallis test. **d**, Survival curves of non-treated and DSS treated C3H/HeJ mice mice infected with WT or *exuR* *C. rodentium*. $N=12$ per group. Log-Rank (Mantel-Cox test) wild-type vs. *exuR* mutant *** $P < 0.0002$ < **** $P < 0.0001$.

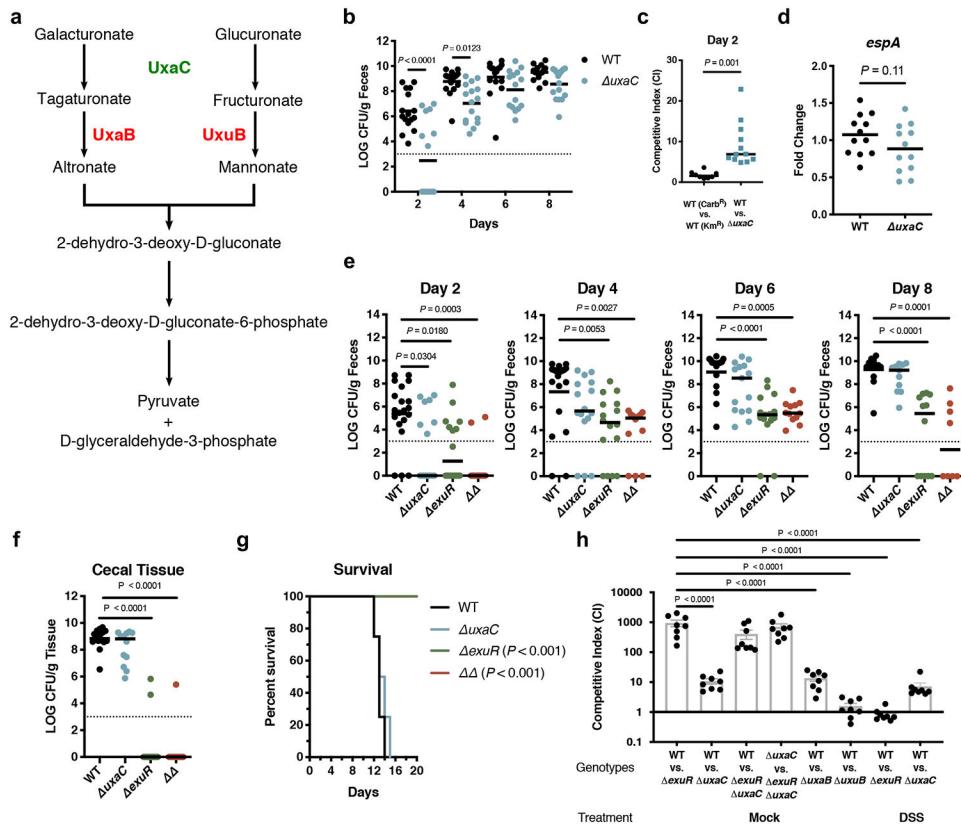


Figure 5]. Regulation of the T3SS by ExuR *in vivo* is independent of its role in regulating galacturonic-acid metabolism.

a, Model depicting a simplified schematic of the Ashwell pathway for galacturonic and glucuronic acid utilization. **b**, Measurement of bacterial CFU from stools of C3H/HeJ mice infected with WT ($n = 16$) or $\Delta uxaC$ ($n = 16$) (n , number of biological replicates; results are representative of two independent experiments). The mean and P value for two-sided two-way ANOVA statistical analysis. **c**, Groups of C3H/HeJ mice were intragastrically inoculated with a 1:1 ratio of the WT (pWSK29; carbenicillin resistant) and WT (pWSK129; kanamycin resistant) ($n = 8$), or WT and $\Delta uxaC$ ($n = 12$) *C. rodentium* strains. Samples were collected 2 days after infection. Competitive indices were calculated using the relative abundance of each strain in the cecal content, corrected by the ratio in the inoculum (n , number of biological replicates; results are representative of two independent experiments). The mean and P value for two-sided Mann-Whitney statistical analysis. **d**, RT-qPCR for LEE-encoded genes *espA* from the cecal content of mice infected with WT ($n = 12$) or $\Delta uxaC$ ($n = 12$) collected 2 days post infection (n , number of biological replicates; results are representative of three independent experiments). The mean and P value for two-sided two-way Mann-Whitney statistical analysis. **e**, Measurement of bacterial CFU from stools of C3H/HeJ mice infected with WT ($n = 12$) or $\Delta uxaC$ ($n = 12$), $\Delta exuR$ ($n = 12$), $\Delta uxaC \Delta uxaR$ ($n = 12$) *C. rodentium* at days 2,4,6 and 8 post-infection (n , number of biological replicates; results are representative of three independent experiments). The mean and P value for two-sided two-way Kruskal-Wallis statistical analysis. **f**, Measurement of bacterial CFU from cecal tissue of C3H/HeJ mice infected with WT ($n = 16$) or $\Delta uxaC$ ($n = 16$), $\Delta exuR$ ($n = 16$), $\Delta uxaC \Delta uxaR$ ($n = 16$) *C. rodentium* 8 days post infection (peak of

disease) (n , number of biological replicates; results are representative of three independent experiments). The mean and P value for two-sided two-way Kruskal-Wallis statistical analysis. **g**, Survival curves of C3H/HeJ mice infected with WT ($n = 8$) or *uxaC* ($n = 8$), *exuR* ($n = 8$), *uxaC uxaR* () ($n = 8$) *C. rodentium*. Statistical significance was calculated using a two-sided log rank (Mantel-Cox) test and P value shown **h**, Competitive indices of C3H/HeJ mice non-treated and treated with DSS infected with equal mixtures of the indicated strains in the cecal content. 2 days after infection, samples were collected for analysis. Values are mean \pm SEM $n = 8$ per group calculated with a two-sided Mann-Whitney statistical test.

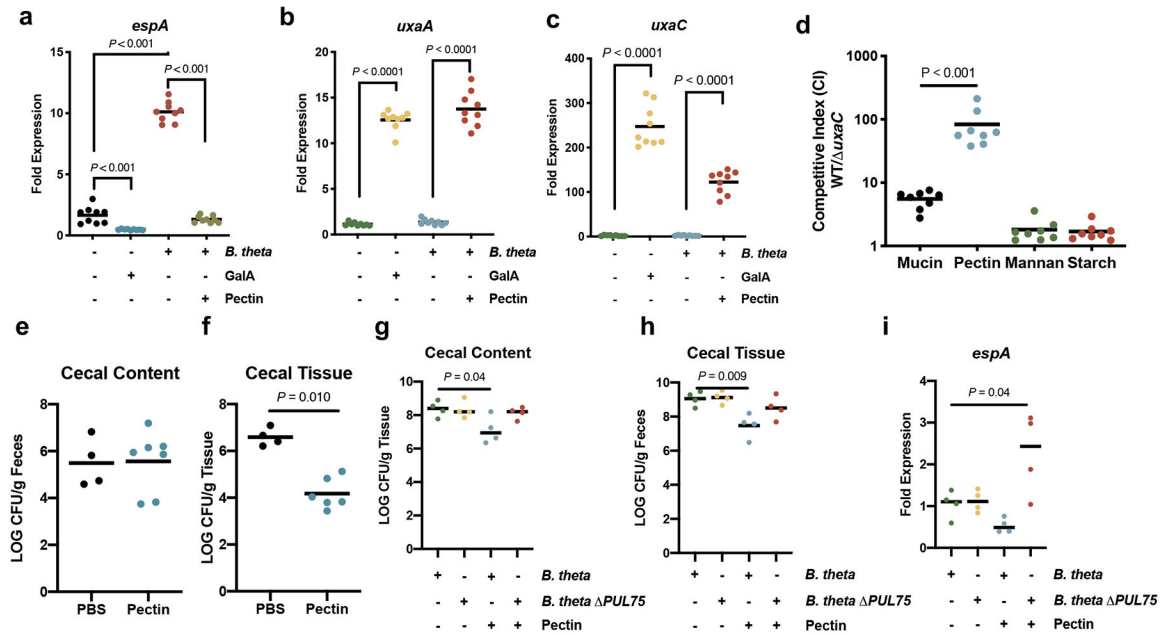


Figure 6]. Dietary pectin is the main source of galacturonic-acid.

a, RT-qPCR for the LEE-encoded gene *espA* **a**, and the sugar acid utilization genes *uxaA* **b**, and *uxaC* **c**, from EHEC co-cultured together with *Bacteroides thetaiotaomicron* in low-glucose DMEM supplemented with 1% of GalA ($n = 8$) or Pectin ($n = 8$) under anaerobic conditions (n , number of biological replicates; results are representative of two independent experiments). The mean and P value for two-sided one-way ANOVA statistical analysis are shown. **d**, *Bt* was grown in *Bacteroides* minimal media with 1% mucin ($n = 8$), starch ($n = 8$), mannan ($n = 8$) or pectin ($n = 8$) as carbon sources. *Bt* was pelleted through centrifugation and the media filtered through a $0.22\mu\text{M}$ filter (pre-conditioned media) (n , number of biological replicates; results are representative of two independent experiments). These media were used for competition assays between WT and *uxaC* *C. rodentium* strains inoculated at 1:1 ratio. The mean and P value for two-sided one-way ANOVA statistical analysis are shown. **e-f**, C57BL/6 mice were infected with *C. rodentium* and treated with $200\mu\text{L}$ of 2% pectin ($n = 4$) or PBS ($n = 4$) for the duration of the experiment (n , number of biological replicates; results are representative of one independent experiments). The mean and P value for two-sided Mann-Whitney statistical analysis are shown. **e**, *C. rodentium* CFU from cecal content. **f**, *C. rodentium* CFU from the cecal tissue. **g-i**, C57BL/6 mice were treated with and antibiotic cocktail to deplete their intestinal microbiota. The mice were subsequently inoculated with WT *Bt* ($n = 4$) or a mutant incapable of breaking down pectin (*Bt* PUL,75) ($n = 4$). After monocolonization the mice were infected with *C. rodentium* and fed a diet including ($n = 4$) or excluding ($n = 4$) pectin (n , number of biological replicates; results are representative of one independent experiments). The mean and P value for two-sided Mann-Whitney statistical analysis are shown. **g**, *C. rodentium* CFU from cecal content. **h**, *C. rodentium* CFU from the cecal tissue. **i**, RT-qPCR for LEE-encoded gene *espA* from the cecal content of mice infected with *C. rodentium*.